THE INFLUENCE OF THE INPUT PARAMETERS SELECTION ON THE RANSAC RESULTS

Urbancic, T.; Kosmatin Fras, M.; Stopar, B. & Koler, B.

University of Ljubljana, Faculty of Civil and Geodetic Engineering, Jamova 2, Ljubljana, Slovenia

E-Mail: tilen.urbancic@fgg.uni-lj.si

Abstract

The RANSAC (RANdom SAmpling and Consensus) enables us to search within a given group of points for subgroups of points that belong to a mathematically describable object or a part of an object. The number of iterations within a single repetition depends on the data, selection and settings of the input parameters (percentage of inliers, probability and minimum number of points that uniquely define a geometrical shape). In our research we applied simulation modelling to analyse the influence of the selection of input parameters on the approximation of the sphere and plane models.

(Received in June 2013, accepted in January 2014. This paper was with the authors 2 months for 1 revision.)

Key Words: RANSAC, Simulation, Input Parameters, Plane Model, Sphere Model

1. INTRODUCTION

Spatial data can be acquired with various technologies. Close range photogrammetry (image matching methods) [1] and terrestrial laser scanning are appropriate [2, 3] when we need to quickly gather large quantities of data in a small area. In both cases the measurement results are points in a 3-D space or point cloud. The quality of the obtained coordinates is evaluated by comparing the parameters of known geometrical shapes that can be recognised within the point cloud. The geometrical shapes can be natural or artificial objects and targets [4]. Various algorithms make it possible to recognise and search for points that belong to a known and mathematically describable geometrical shape (e.g. plane, sphere). The most commonly used approaches are the Hough transform [5] and the RANSAC (RANdom SAmpling and Consensus) method [6].

The RANSAC can be used in a variety of fields. The method developers, Fischler and Bolles [6], used it for defining the parameters of the external orientation of a photogrammetric image. It is also used in medicine [7, 8], robotics [9, 10], computer vision [11, 12], image matching [13] and engineering [14]. In geodesy it is used for segmentation and registration of laser scanning point clouds [15-17], satellite images registration [18, 19] and improvement of the transformation parameters estimates between two coordinate systems [20, 21].

The RANSAC is used to define the point cloud's subgroup that includes the highest number of points from the original cloud for the selected threshold value and mathematical model. The number of iterations for a single repetition depends on the percentage of inliers, probability and the minimum number of points that mathematically describe the object model. The algorithm is based on a random selection of the minimum number of points that define the mathematical model of the object. When performing multiple repetitions we can thus obtain somewhat different results or different object model even when identical input parameters are used.

We used the RANSAC to analyse the influence of the threshold value and percentage of inliers on the number of points in the subgroup that represents the model of the plane and sphere for a selected (constant) probability, at a high number of independent calculation repetitions. Applying simulation modelling we have also analysed how the changes in the threshold value influence the parameters that define the two geometrical models. The point

cloud obtained from terrestrial laser scanning was used as test data.

2. RANSAC

The RANSAC helps define the subgroup of points S^* within a given point cloud S, in which a maximum number of points fit the geometrical model (Fig. 1). The search for the optimum subgroup S^* uses a minimum number of randomly selected points m that belong to subgroup S_k and uniquely define the geometrical shape to create a mathematical model M_k of the selected geometrical shape. The second step verifies how many of the remaining cloud points belong to the model when we take into account a previously set threshold value t. In the search for points that belong to S^*, the orthogonal distances $\delta_k(s)$ of the point in point cloud S from the mathematical model M_k are compared. The appropriateness of the selected model is evaluated by the number of points in a subgroup S_k^*. The process is repeated N times and we select the subgroup S^* in which the number of points or inliers n is the highest [6].

Input parameters for the algorithm are: m – minimum number of points needed to define the model; w – percentage of inliers in the point cloud; p – the probability that the best fitting model in one of the iterations is found; t – threshold value is the distance of points in a cloud that still belong to the selected model; S – data or point cloud.

Determine a number of iterations N

$$N = \frac{\log(1-p)}{\log(1-w^m)}$$

The result of algorithm is the set S^* from S_k^* which contains the maximal number of point

$$S^* = \left\{ S_k^* \mid \|S_k^*\| = \max_{k=1,\dots,N} \|S_k^*\| \right\}$$

for $k = 1, \dots, N$
1. Randomly pick m points from $S \rightarrow S_k$
2. From S_k determine the parameters of mathematical model M_k
3. Select points that are within the tolerance from the mathematical model

$$S_k^* = \left\{ s \mid s \in S \setminus S_k \wedge \delta_k(s) \le t \right\}$$
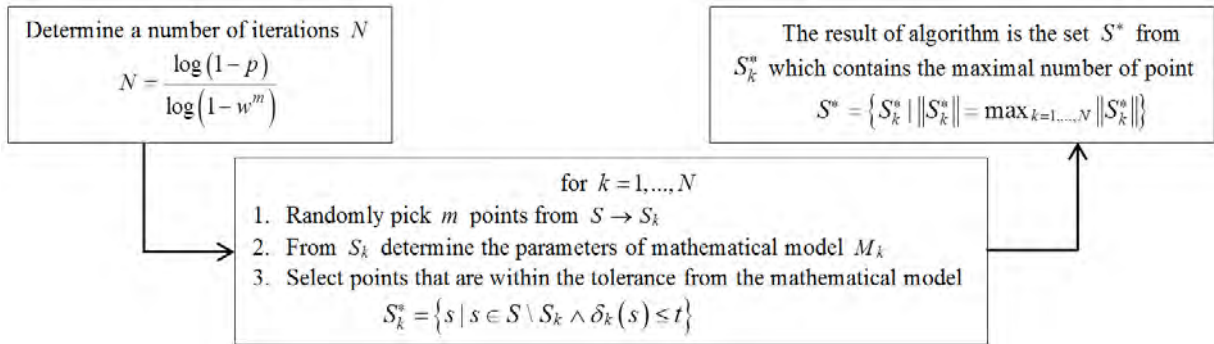
Figure 1: The RANSAC algorithm.

The number of iterations N (eq. (2)) depends on the lowest number of points m that uniquely define the model, the percentage of inliers w and the selected probability p. The chosen probability p is the probability that the model M_k is defined from S_k with which the selected geometrical shape is found at least in one repetition. In this case w^m represents the probability that all points within the subgroup S_k are inliers. From this we can conclude that $1 - w^m$ is the probability that at least one of the points in subgroup S_k is an outlier. If we perform N repetitions there is a $(1-w^m)^N$ possibility that at least one repetition in group S_k will include an outlier. The probability that the algorithm never choses solely inliers is thus the same [6]:

$$1 - p = \left(1 - w^m\right)^N \tag{1}$$

With the lowest number of points m that uniquely define the selected geometrical shape, chosen probability p and the assumption of value w we can obtain parameter N by applying the logarithm to the eq. (1):

$$N = \frac{\log(1-p)}{\log(1-w^m)} \tag{2}$$

The influence of the number of iterations on the result of the RANSAC algorithm will be discussed in our search for points on the models of the plane and sphere.

2.1 Setting the plane and sphere models

We will test the influence of the input parameters for both geometrical shapes that comprise the test field. The plane is uniquely defined by three non-collinear points. The equation can be written as:

$$ax + by + cz - d = 0 \tag{3}$$

in which a, b, c and d are parameters of the plane, x, y and z are the coordinates of the points on the plane. For each point in S we calculate the perpendicular distance δ_i of point i from the mathematical plane model that is calculated with the following equation:

$$\delta_i = \frac{|a \cdot x_i + b \cdot y_i + c \cdot z_i - d|}{\sqrt{a^2 + b^2 + c^2}} \tag{4}$$

When defining the plane with the RANSAC we treat all points in which $|\delta_i| < t$ as inliers. As we have already mentioned these points belong to subgroup S^*.

The sphere is uniquely defined by four non-coplanar points on its surface. The equation of the sphere can be written as follows:

$$(x - x_C)^2 + (y - y_C)^2 + (z - z_C)^2 - r^2 = 0 \tag{5}$$

in which x, y and z are coordinates of the points on the sphere, x_C, y_C and z_C are the coordinates of the centre and r is the radius of the sphere. For each point in S we once again calculate the perpendicular distance δ_i from the mathematical model of the sphere which we calculate with the equation $\delta_i = \xi_i - r$. ξ_i represents the distance of point i from the sphere centre. Similar as was the case with the plane, points in which $|\delta_i| < t$ belong to subgroup S^*.

3. RESEARCH METHODOLOGY

We evaluate the influence the changes of the percentage of inliers w and threshold value t have on the number of points in subgroup S^* when using the RANSAC. A high number of independent repetitions of the calculation were performed with a simulation of random t values. Subgroup S^* includes the highest possible number of points belonging to the model at which the threshold value was used. A subgroup of points defined in this way represents the basis for defining the most likely value of the parameters of the geometrical shape, which is then approximated with the least square method (LSM) (Fig. 2) [22, 23]. With the approximation of the geometrical shapes we obtain different parameters.

TEST DATA: terrestrial laser scanning point cloud	PLANE: changes of parameters a, b, c and d
↓	SPHERE: changes of sphere radius R
RANSAC - simulation of 10000 repetitions of the calculation independent values for 0.5 mm $\leq t \leq$ 3.5 mm - $p = 99\,\%$ - $m = 3$ for the plane, $m = 4$ for the sphere - $w = 99\,\%$, 90 %, 80 %, 70 %, 60 %, 50 %	least square method (LSM) ↑
	RANSAC RESULTS - 10000 subgroups S^* - changes of n in S^* into account the t
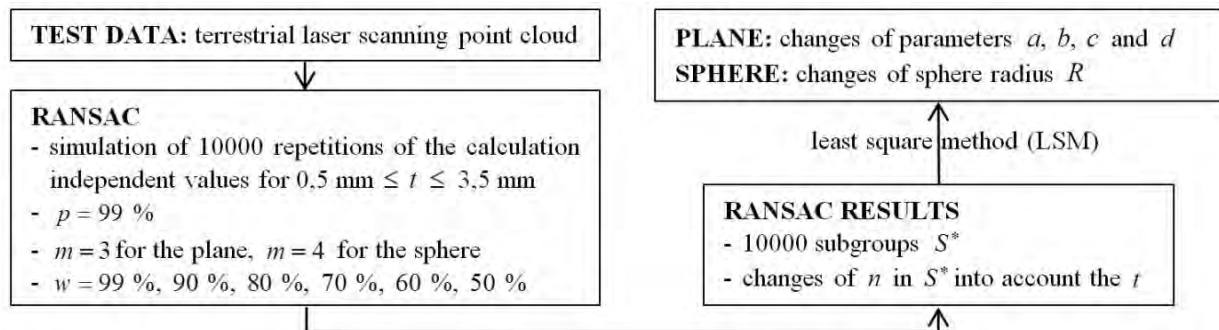
Figure 2: Schematic representation of the research.

The influence the change in the number of inliers has on the results of the RANSAC and the estimated parameters of the geometrical shapes was analysed with 10000 repetitions of the

calculation. The procedure was repeated for each inlier's percentage w, in which we used a simulation to define the random threshold value between (and including) 0.5 and 3.5 mm. We performed this test on terrestrial laser scanning data obtained with a Riegl VZ-400 scanner at a distance of 10 m with resolution 2 mm × 2 mm. The lower and upper threshold values were defined on the basis of the test calculations and the preciseness of the point's coordinates, which depends on the precision of the instrument [24] and the scanning distance.

The scanned test field is composed of the plane and the semi-sphere which are commonly used geometrical shapes for point cloud registration and segmentation [2, 15-17] and calibrating measurement systems [25]. The radius of the semi-sphere (49.70 mm ± 0.05 mm) was measured with callipers. Prior to the calculations the point cloud was composed of certain number of points that belonged to the model (inliers) and a selected percentage of outliers (Table I and Fig. 3).
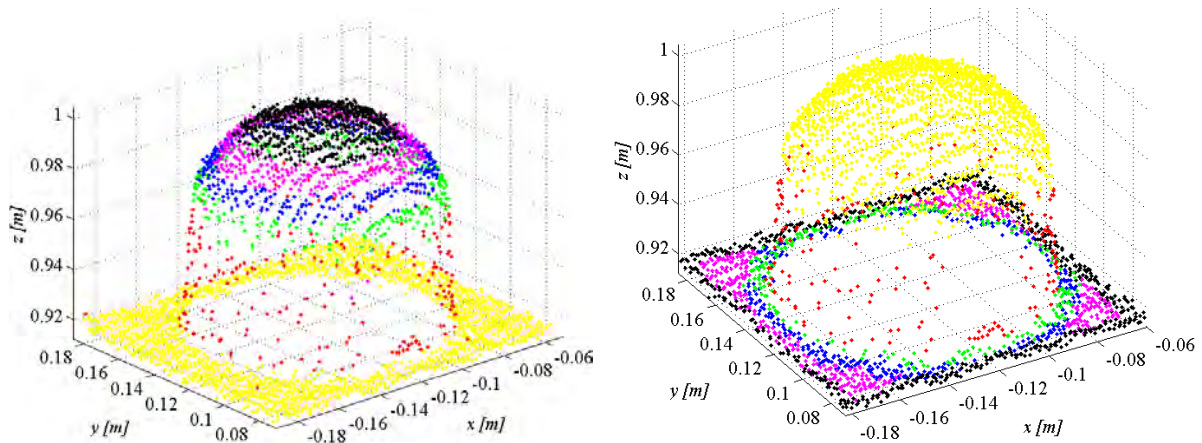
Figure 3: Test field point cloud: plane (left), sphere (right).

Table I: Number of points and number of iterations in one repetition of the RANSAC.

Attempt	Colour*	Inliers		Outliers		No. of all points		Inliers [%]	Outliers [%]
		plane	sphere	plane	sphere	plane	sphere		
1	Y	2040	1822	20	18	2060	1840	99	1
2	YR	2040	1822	227	202	2267	2024	90	10
3	YRG	2040	1822	510	456	2550	2278	80	20
4	YRGB	2040	1822	874	781	2914	2603	70	30
5	YRGBM	2040	1822	1360	1215	3400	3037	60	40
6	YRGBMK	2040	1822	2040	1822	4080	3644	50	50

* Y – yellow, R – red, G – green, B – blue, M – magenta and K – black.

4. TESTING AND RESULT ANALYSIS

In accordance to the described methodology we analysed six combinations (attempts 1 to 6) of inliers' percentage. In each attempt we had a different percentage of inliers and a different number of iterations. In each repetition of our search the RANSAC performed a number of iterations N, which was defined by eq. (2) and is shown in Table II. We did not change the probability levels, which was in all cases $p = 99$ %, nor did we change the minimum number of points m ($m = 3$ for the plane and $m = 4$ for the sphere).

Table II: Number of iterations according to the various percentages of inliers w.

Attempt		1	2	3	4	5	6
w [%]		99	90	80	70	60	50
N	plane	1	4	6	11	19	34
N	sphere	1	4	9	17	33	71

4.1 The analysis of the plane results

The simulation of 10000 independent repetitions of the calculation enables the analysis of the threshold value t. Within the simulation every one of the 10000 repetitions gave us the best subgroup S^* of the original point cloud S. Fig. 4 shows the changes in the number of points n in S^*, at which it takes into account the randomly selected threshold value t for all 6 attempts performed for the plane model.
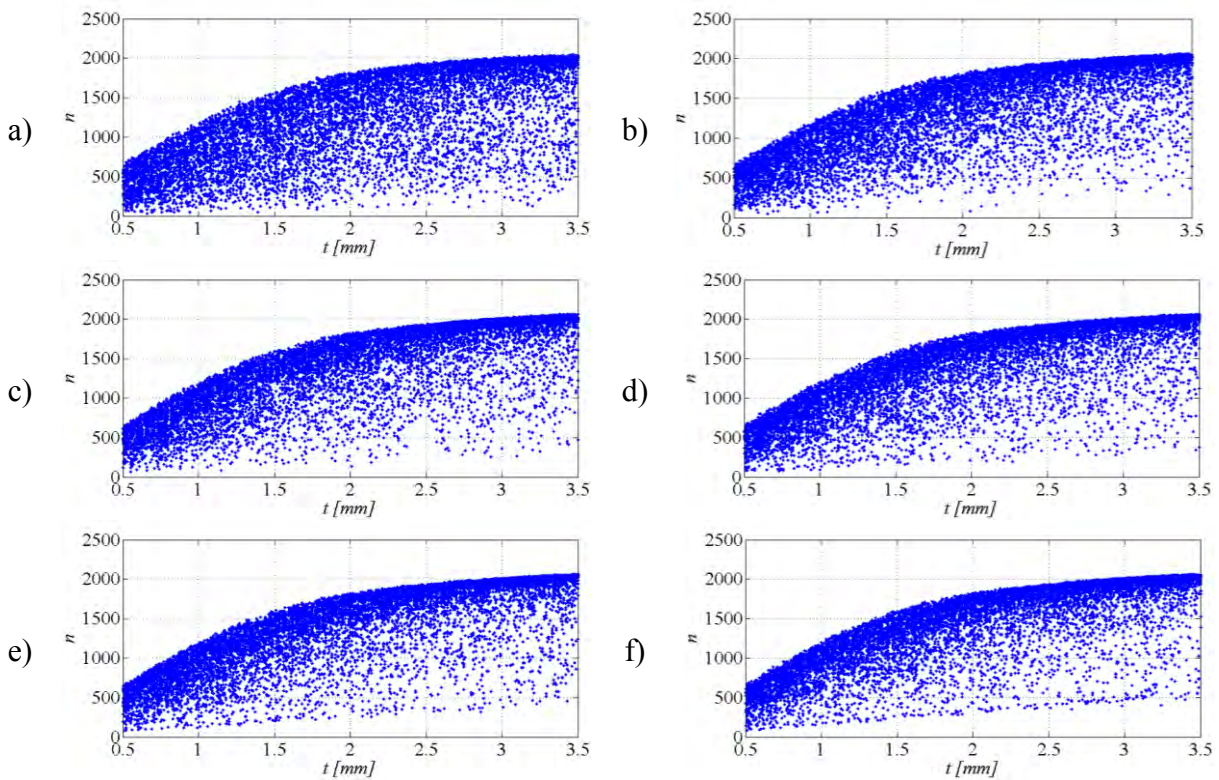
Figure 4: Number of points n in S^* in relation to t, for the plane; a) attempt 1, b) attempt 2, c) attempt 3, d) attempt 4, e) attempt 5, and f) attempt 6.

All six attempts resulted in a similar shape of the area within which the results of all repetitions can be found (Fig. 4). This area is limited by a curve (parabola) on the upper part and a line on the lower part. By adding outliers the number of iterations N increased, which led to an increase in the density of points on the upper border of the area. As an example the histograms of the number of points n in S^* (Fig. 5) are shown for attempts 1 and 6 (highest and lowest w value). Even though the number of outliers in S increased, the higher number of repetitions of the calculation with the use of the RANSAC provided better results for attempt 6 when compared to attempt 1 (Figs. 4 and 5). A similar conclusion was reached in the analysis of the dispersion of the plane parameters (Fig. 6). The dispersed results were reduced when the threshold value t and the percentage of outliers were increased. This example leads to the conclusion that the quality of the search for points that belong to the plane is influenced by the number of iterations rather than the percentage of outliers (Figs. 4 and 6).
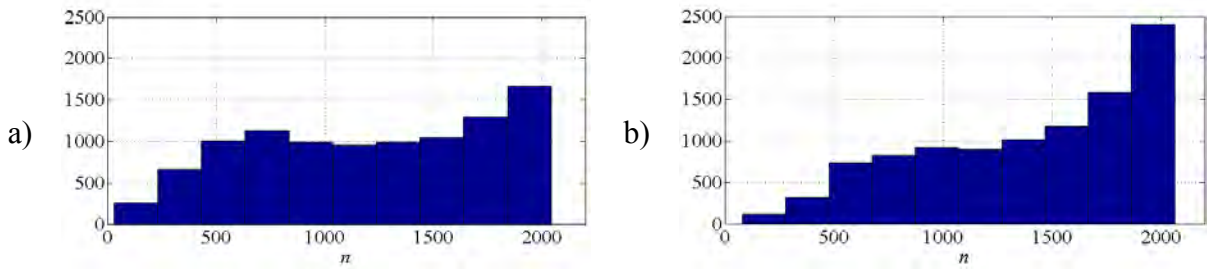
Figure 5: Histograms of the number of points n in S^*, for the plane; a) attempt 1, b) attempt 6.
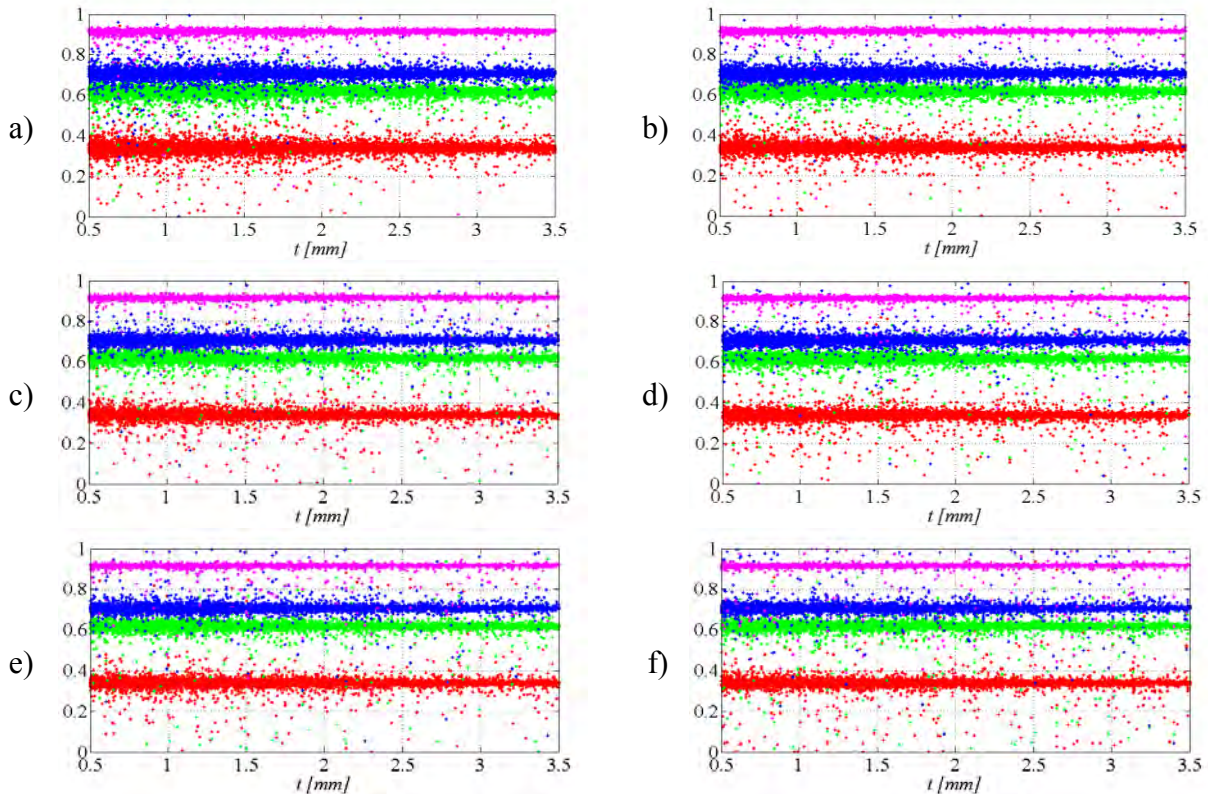
Figure 6: Plane parameters: a – red, b – green, c – blue, d – magenta; a) attempt 1,
b) attempt 2, c) attempt 3, d) attempt 4, e) attempt 5, and f) attempt 6.

4.2 Analysis of the sphere results

We applied the same procedure to the sphere. Fig. 7 shows the changes in the number of points n in S^* in relation to threshold value t for 6 different examples of inlier percentages. Figs. 7 a) to 7 f) show that the number of points n in S^* varied greatly in all 6 cases. On the right hand side of the individual graphs in Figs. 7 c) to 7 f) we can see that some solutions provide groups of points that include more points than the sphere model. As a result of the calculations the algorithm thus offers a subgroup of points that includes outliers. The reason lies in a threshold value that was set too high. Correct results were obtained for the threshold value $t < 2.5$ mm, as the results for $t > 2.5$ mm included a higher number of points than actually belong to the sphere. The area in which we can find the correct results of the number of points n in S^* is limited on the upper side with a curve (parabole), and on the lower side with a line.

Further on we used subgroup S^* as the base for our estimate of the sphere parameters (coordinates of the centre and the radius).
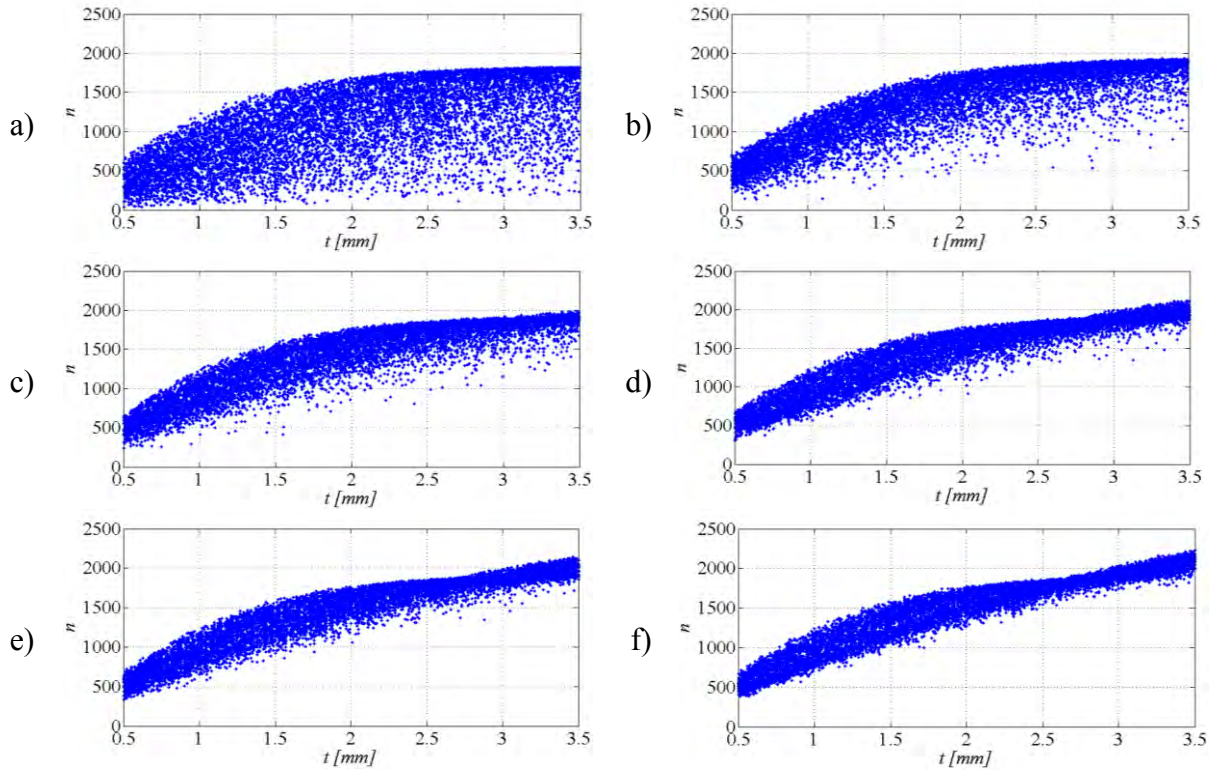
Figure 7: Number of points n in S^* in relation to threshold value t, for the sphere;
a) attempt 1, b) attempt 2, c) attempt 3, d) attempt 4, e) attempt 5, and f) attempt 6.
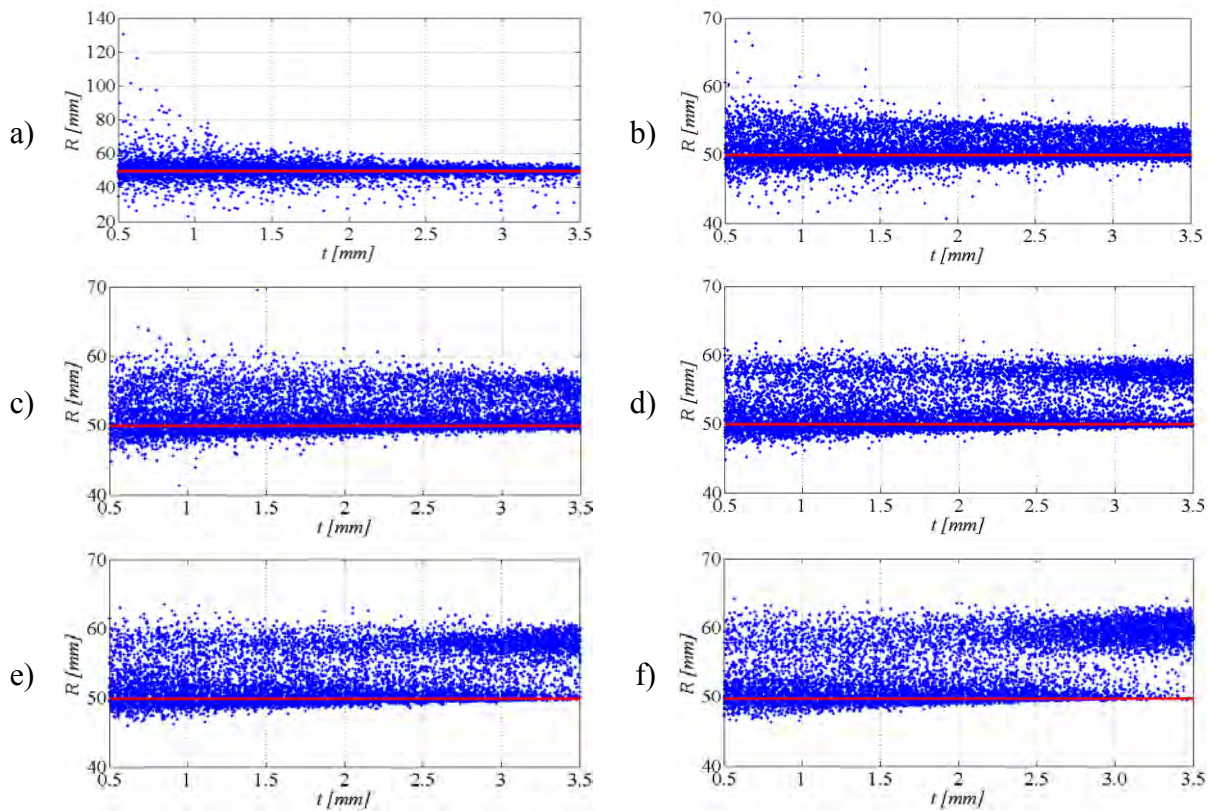
Figure 8: Sphere. Dispersion of the results of sphere radius R in relation to threshold value t;
a) attempt 1, b) attempt 2, c) attempt 3, d) attempt 4, e) attempt 5, and f) attempt 6.

Fig. 7 shows that the number of points *n* has changed greatly in relation to threshold value *t*. This also influences the results of the approximate shape of the sphere to which these points belong. Fig. 8 shows the changes in the radius of the approximate sphere in relation to *t*; the true value of the radius (49.70 mm) is shown by the red line.
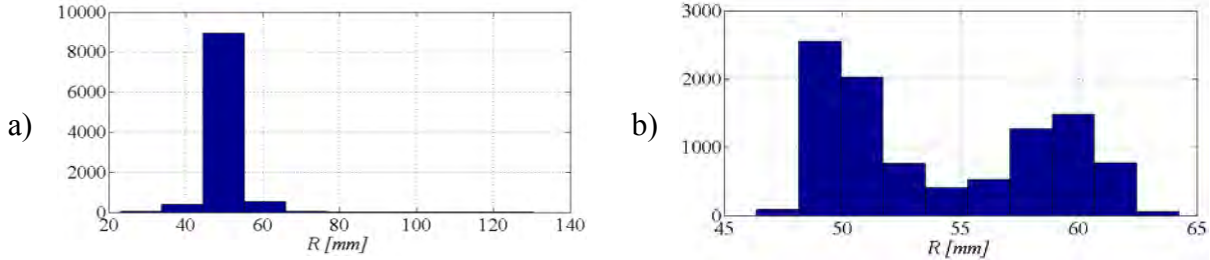
Figure 9: The histogram of defining the sphere radius *R*; a) attempt 1, b) attempt 6.

The histogram for attempt 1 shows that with the probability of 99 % the correct result was reached in somewhat less than 90 % of the repetitions. In attempt 6 this percentage was much lower (Fig. 9).

Let's take a look at an example of a solution for a sphere for which the radius was correctly and incorrectly defined. Table III shows the data on the number of points *n* in subgroup S^*, a randomly generated threshold value *t*, coordinates of the centre and the sphere radius for the two solutions in attempt 6. The results are also shown in the form of a cross-section of the sphere and plane $y = 0$ (Fig. 10).
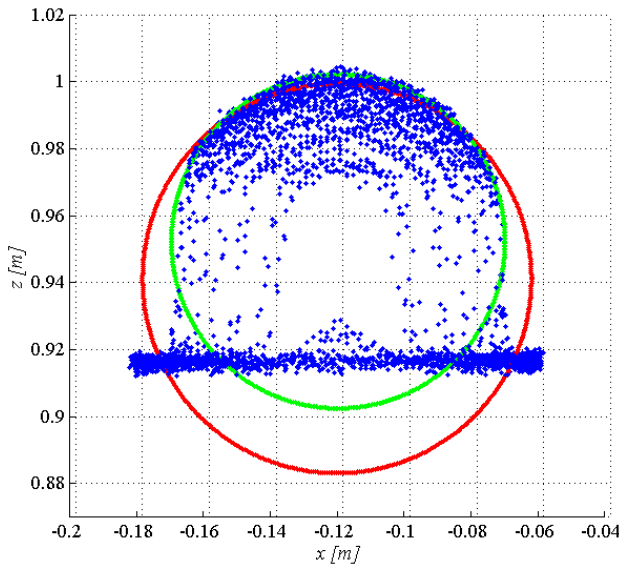
Figure 10: The approximated sphere is shown as a cross section with plane $y = 0$, the point cloud is depicted in blue, the correct result in green and the incorrect result in red.

Table III: The two solutions in attempt 6.

n	*t*	*x* [m]	*y* [m]	*z* [m]	*R* [mm]
2094	3.42	-0.12118	0.12765	0.94127	58.11
1552	1.60	-0.12080	0.12760	0.95237	49.76

The influence the outliers have on the calculation of the coordinates of the centre and the sphere radius cannot be overlooked. In the two compared cases the spatial distance between the coordinates of the centre amounts 11.11 mm. The radii differ by 8.35 mm.

4.3 The percentage of inliers is underestimated

So far we have ascertained that the actual number of correct solutions, regardless of the demanded probability level of 99 %, is lower than expected. We were further interested to explore the change of the inliers percentage so that we intentionally increase the number of iterations within a single repetition. We studied the points in attempt 1 ($w = 99$ %) and attempt 4 ($w = 70$ %); in both cases we intentionally reduced the percentage of inliers to $w = 50$ % thus the number of iterations also changed. In attempt 1 the algorithm performed 34 iterations instead of 1 for the plane and 71 iterations instead of 1 for the sphere.

In search for the plane model there is a large change in the distribution of the number of points n in subgroup S^*. Most solutions came close to the upper edge of the area (Fig. 11 a). A lesser dispersion was noticed for the estimated values of the plane parameters (Fig. 11 b). A similar ascertainment can be reached when searching for the model of the sphere (Fig. 12). The figures show a change in the number of points n in S^* and the sphere radius R.
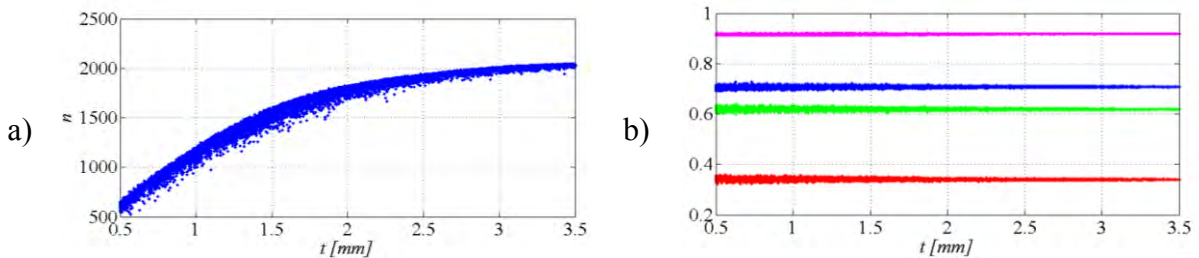
Figure 11: a) number of points n in S^* and b) parameters of the plane in relation to threshold value t for attempt 1, with a reduced percentage of inliers $w = 50$ %.
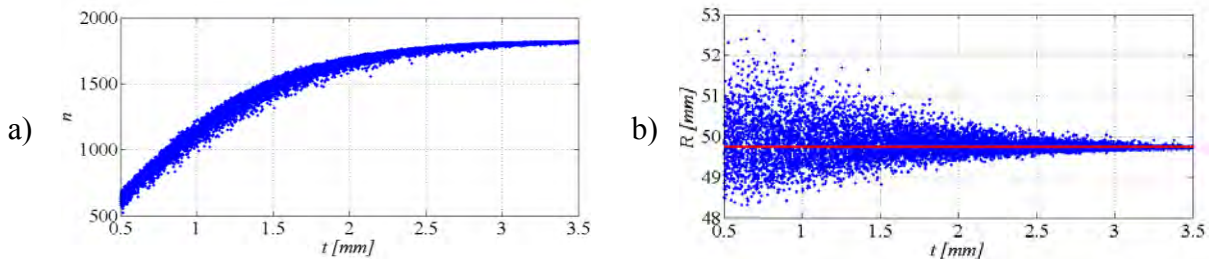
Figure 12: a) number of points n in S^* and b) radii of the sphere R in relation to threshold value t for attempt 1, with a reduced percentage of inliers $w = 50$ %.

In the second test case within attempt 4 the number of iterations for the plane increased from 11 to 34 and for the sphere from 17 to 71. For the plane the number of iterations was artificially increased by 309 %. By comparing the results without increasing the numbers of iterations N (Figs. 4 d and 6 d) we obtained much better results with 34 iterations (Fig. 13). The number of points n moved closer towards the upper edge of the area, which means that the solutions do not deviate as much from each another (Fig. 13 a). Similar can be said for the parameters of the plane. In both cases the dispersion of the estimated parameters of the sphere and plane is much lower (Fig. 13 b).

Even though we increased the number of iterations in our search for the points of the sphere by 417 %, we still obtained subgroups S^* that included outliers (Fig. 14). In most cases the size of the threshold value $t > 2.5$ mm led to an incorrect solution of the sphere model.

By intentionally reducing the percentage of inliers we increased the number of iterations in a single repetition. This intervention into the algorithm resulted in a smaller area of result dispersion, i.e. number of points n in S^* and the parameters of the models (Figs. 13 and 14).
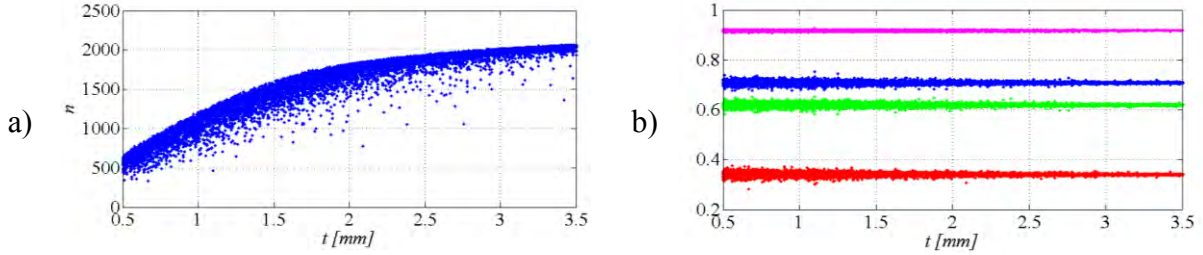
Figure 13: a) number of points n in S^* and b) parameters of the plane in relation to threshold value t for attempt 4, with a reduced percentage of inliers $w = 50$ %.
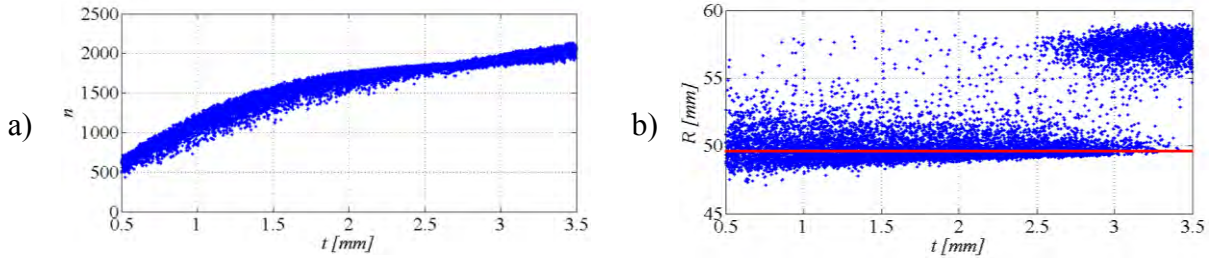
Figure 14: a) number of points n in S^* and b) radii of the sphere R in relation to threshold value t for attempt 4, with a reduced percentage of inliers $w = 50$ %.

5. CONCLUSION

Despite the relatively rich literature of the use of RANSAC we have not found a research in which the authors would attempt to evaluate the quality of the obtained results. Applying simulation modelling in our research we wished to ascertain the influence and importance of selecting correct input parameters. We tested how changes in the percentage of inliers w and threshold value t influence the results given by the RANSAC and how this effects the parameters of the geometric shapes following the LSM approximation using the results of the simulated (randomly selected) values of threshold value t. We found out that the dispersion or size of the area of solutions for the number of points n in S^* varies greatly in the various combinations of the estimated percentage of inliers w and threshold value t. We also analysed the dispersion of the estimated parameters of the geometrical shapes. We concluded that in order to achieve a correct result we need efficient information on the treated point cloud and a correct estimate of the percentage of inliers w and the threshold value t.

We realised that we did not always obtain a percentage of correct results as high as one would expect despite correctly estimated t, w and p. In the case of low t values there is a great dispersion of results (radii and plane parameters) in all cases. We estimated that for a sphere the highest percentage of correct results is for the threshold value $1.5 \leq t \leq 2.5$ mm. In the case of the plane the selection of the threshold value was of lesser significance for the dispersion.

With intentional increases in the number of iterations or an incorrect estimation of the percentage of inliers we have shown that the dispersion of the results is reduced. With the RANSAC we can simply and quickly find the subgroup of points that is best fitted to the geometrical shape, however, in order to confirm the obtained results we need to repeat the calculations several times. The quality of the results obtained by the RANSAC depends to a great extent on the previous treatment of the point cloud. Regardless of the carefully selected and correctly set input parameters (especially the percentage of inliers and threshold value), it is advisable to verify the results with multiple independent repetitions of the calculation.

6. ACKNOWLEDGEMENTS

REFERENCES

[1] Peterman, V.; Mesaric, M. (2012). Land survey from unmanned aerial vehicle, *International Archives of the Photogrammetry, Remote Sensing and Spatial Information Sciences,* Vol. XXXIX-B1, *XXII ISPRS Congress*, Melbourne, 447-451, doi:10.5194/isprsarchives-XXXIX-B1-447-2012

[2] Arias, P.; Arnesto, J.; Lorenzo, H.; Ordonez, C. (2007). 3D terrestrial laser technology in sporting craft 3D modelling, *International Journal of Simulation Modelling*, Vol. 6, No. 2, 65-72, doi:10.2507/IJSIMM06(2)S.01

[3] Vezocnik, R.; Ambrozic, T.; Sterle, O.; Bilban, G.; Pfeifer, N.; Stopar, B. (2009). Use of terrestrial laser scanning technology for long term high precision deformation monitoring, *Sensors*, Vol. 9, No. 12, 9874-9895, doi:10.3390/s91209873

[4] Urbancic, T.; Koler, B.; Stopar, B.; Kosmatin Fras, M. (2014). Analiza kakovosti določitve parametrov krogle pri terestričnem laserskem skeniranju = Quality analysis of the sphere parameters determination in terrestrial laser scanning, *Geodetski vestnik,* Vol. 58, No. 1, 11-27

[5] Tarsha-Kurdi, F.; Landes, T.; Grussenmeyer, P. (2007). Hough-transform and extended RANSAC algorithms for automatic detection of 3D building roof planes from Lidar data, *ISPRS Workshop on Laser Scanning 2007 and SilviLaser 2007*, Espoo, Vol. XXXVI, Part 3/W52, 407-412

[6] Fischler, M. A.; Bolles, R. C. (1981). Random sample consensus: a paradigm for model fitting with applications to image analysis and automated cartography*, Communications of the ACM*, Vol. 24, No. 6, 381-395, doi:10.1145/358669.358692

[7] Zhao, Y.; Liebgott, H.; Cachard, C. (2012). Tracking biopsy needle using Kalman filter and RANSAC algorithm with 3D ultrasound, *Proceedings of the Acoustics 2012 Nantes Conference*, Nantes, 231-236

[8] Wang, M. H.; Palmeri, M. L.; Rotemberg, V. M.; Rouze, N. C.; Nightingale, K. R. (2010). Improving the robustness of time-of-flight based shear wave speed reconstruction methods using RANSAC in human liver in vivo, *Ultrasound in Medicine and Biology*, Vol. 36, No. 5, 802-813, doi:10.1016/j.ultrasmedbio.2010.02.007

[9] Maier, J.; Humenberger, M. (2013). Movement detection based on dense optical flow for unmanned aerial vehicles, *International Journal of Advanced Robotic Systems*, Vol. 10, 11 pages, doi:10.5772/52764

[10] Papazov, C.; Haddadin, S.; Parusel, S.; Krieger, K.; Burschka, D. (2012). Rigid 3D geometry matching for grasping of known objects in cluttered scenes, *The International Journal of Robotics Research*, Vol. 31, No. 4, 538-553, doi:10.1177/0278364911436019

[11] Liu, J.; Wark, T.; Lakemond, R.; Sridharan, S. (2012). Self-calibration of wireless cameras with restricted degrees of freedom, *Computer Vision and Image Understanding*, Vol. 116, No. 10, 1033-1046, doi:10.1016/j.cviu.2012.06.001

[12] Jimenez, P.; Bergasa, L. M.; Nuevo, J.; Alcantarilla, P. F. (2012). Face pose estimation with automatic 3D model creation in challenging scenarios, *Image and Vision Computing,* Vol. 30, No. 9, 589-602, doi:10.1016/j.imavis.2012.06.013

[13] Weinmann, Ma.; Weinmann, Mi.; Hinz, S.; Jutzi, B. (2011). Fast and automatic image-based registration of TLS data, *ISPRS Journal of Photogrammetry and Remote Sensing*, Vol. 66, No. 6, S62-S70, doi:10.1016/j.isprsjprs.2011.09.010

[14] Naranbaatar, E.; Kim, H.-S.; Lee, B.-R. (2012). Radius measuring algorithm based on machine vision using iterative fuzzy searching method, *International Journal of Precision Engineering and Manufacturing,* Vol. 13, No. 6, 915-926, doi:10.1007/s12541-012-0119-y

[15] Tittmann, P.; Shafii, S.; Hartsough, B.; Hamann, B. (2011). Tree detection, delineation, and measurement from LiDAR point clouds using RANSAC, *Proceedings of SilviLaser 2011 – 11th International Conference on LiDAR Applications for Assessing Forest Ecosystems*, Hobart, 583-595

[16] Theiler, P. W.; Schindler, K. (2012). Automatic registration of terrestrial laser scanner point clouds using natural planar surfaces, *ISPRS Annals of Photogrammetry, Remote Sensing and Spatial Information Sciences*, Vol. I-3, *XXII ISPRS Congress*, Melbourne, 173-178, doi:10.5194/isprsannals-I-3-173-2012

[17] van der Sande, C.; Soudarissanane, S.; Khoshelham, K. (2010). Assessment of relative accuracy of AHN-2 laser scanning data using planar features, *Sensors*, Vol. 10, No. 9, 8198-8214, doi:10.3390/s100908198

[18] Kim, T.; Im, Y-J. (2003). Automatic satellite image registration by combination of matching and random sample consensus, *IEEE Transactions on Geoscience and Remote Sensing*, Vol. 41, No. 5, 1111-1117, doi:10.1109/TGRS.2003.811994

[19] Oh, J.; Toth, C. K.; Grejner-Brzezinska, D. A. (2010). Automatic georeferencing of aerial images using high-resolution stereo satellite images, *Proceedings of the ASPRS Annual Conference,* San Diego, 714-729

[20] Brown, M.; Lowe, D. (2002). Invariant features from interest point groups, *Proceedings of the British Machine Vision Conference*, Cardiff, 253-262, doi:10.5244/C.16.23

[21] Barnea, S.; Filin, S. (2007). Registration of terrestrial laser scans via image-based features, *ISPRS Workshop on Laser Scanning 2007 and SilviLaser 2007*, Espoo, Vol. XXXVI, Part 3/W52, 32-37

[22] Grigillo, D.; Stopar, B. (2003). Metode odkrivanja grobih pogreškov v geodetskih opazovanjih = Methods of gross error detection in geodetic observations, *Geodetski vestnik*, Vol. 47, No. 4, 387-403

[23] Kuang, S. (1996). *Geodetic network analysis and optimal design: Concepts and applications*, Ann Arbor Press, Chelsea

[24] RIEGL Laser Measurement Systems. RIEGL VZ-400, from *http://riegl.com/nc/products/terrestrial-scanning/produktdetail/product/scanner/5/*, accessed on 09-10-2013

[25] Acko, B.; McCarthy, M.; Haertig, F.; Buchmeister, B. (2012). Standards for testing freeform measurement capability of optical and tactile coordinate measuring machines, *Measurement Science and Technology*, Vol. 23, No. 9 (Article number: 094013), 13 pages, doi:10.1088/0957-0233/23/9/094013